Shedding light on the use of Cu(II)-salen complexes in the A^3 coupling reaction

Stavroula I. Sampani,[a] Victor Zdorichenko,[b] Marianna Danopoulou,[a] Matthew C. Leech,[c] Kevin Lam,[c] Alaa Abdul-Sada,[a] Brian Cox,[a,b] Graham J. Tizzard,[d] Simon J. Coles,[d] Athanassios Tsipis[e] and George E. Kostakis[a*]

[a]Department of Chemistry, School of Life Sciences, University of Sussex, Brighton BN1 9QJ, UK. E-mail: G.Kostakis@sussex.ac.uk

[b]Photodiversity Ltd c/o Department of Chemistry, School of Life Sciences, University of Sussex, Brighton BN1 9QJ, UK.

[c]School of Science, Department of Pharmaceutical Chemical and Environmental Sciences, University of Greenwich, Central Avenue, Chatham Maritime, ME4 4TB, UK.

[d]UK National Crystallography Service, Chemistry, University of Southampton, SO1 71BJ, UK.

[e]Laboratory of Inorganic and General Chemistry, Department of Chemistry, University of Ioannina, 451 10 Ioannina, Greece.

Abstract

One Cu(II) complex, {Cu(II)L} (**1S**), has been synthesised, in two high yielding steps under ambient conditions, and characterised by single-crystal X-Ray diffraction (SXRD), IR, UV-Vis, Circular Dichroism (CD), Elemental analysis, Thermogravimetric analysis (TGA) and Electron Spray Ionization Mass Spectroscopy (ESI-MS). This air-stable compound enables the generation, at room temperature and open-air, of twenty propargylamines, nine new, from secondary amines, aliphatic aldehydes and alkynes with a broad scope with yields up to 99%. Catalyst loadings can be as low as 1 mol%, while the recovered material retains its structural integrity and can be used up to 5 times without loss of its activity. Control experiments, SXRD,

cyclic voltammetry and theoretical studies shed light on the mechanism revealing that the key to success is the use of phenoxido salen based ligands. These ligands orchestrate topological control permitting alkyne binding with concomitant activation of the C–H bond and simultaneously acting as template temporarily accommodating the abstracted acetylenic proton, and continuous generating, via in-situ formed radicals and Single Electron Transfer (SET) mechanism, of a transient Cu(I) active site to facilitate this transformation. The scope and limitations of this protocol are discussed and presented.

Introduction

The discovery of atom/energy-efficient and low-cost catalytic processes has been a longstanding goal for synthetic chemists; thus, various sophisticated approaches, including multicomponent reactions, have been developed.[1] These methodologies dominate synthetic chemistry because they yield products from simple starting materials, in fewer steps, and in a shorter time. However, the significant challenges of these protocols are to identify a) the appropriate catalyst to promote a specific transformation, b) the suitable combination of functional groups and c) their scope and synthetic versatility. The multi-component reaction of aldehydes, amines and alkynes, known as the A^3 coupling, is a vital route to propargyl amines.[2–7] These organic scaffolds are essential intermediates in the synthesis of biologically active nitrogen-containing compounds, such as acrylamidines, oxazoles, pyrroles, pyrrolidines and natural products.[2–4] Remarkably, few enantioselective A^3 methodologies are known,[8,9] and even fewer are known in which the role of the catalyst is well understood.[10] From these studies, it is established that the aldehyde and amine combine to form an iminium ion, which in turn reacts with the alkyne to yield the product. In light of this, various metal-based methodologies, for example, Au(I)/Au(III),[11–13] Ag(I),[14–17] Cu(I),[18–22] or Rh(III),[23] that facilitate the formation of the corresponding metal acetylide have been developed. However, other transition elements such as Cu(II)[24–26] and Fe(III),[27–29] have also been used, although with higher catalyst loadings and less mechanistic evidence.

Copper is abundant, of low cost, has incredibly versatile chemistry and its oxidation state varies (I, II and III) while its components can catalyse reactions that incorporate one and/or two-electron (radical and bond-forming) based mechanisms. Most importantly, copper easily coordinates to heteroatoms and forms π-bonds to organometallic intermediates, which may be a key step of the observed transformation.[30–32] Unquestionably, the A^3 protocols that incorporate Cu(I) require inert conditions. Work by Li,[33] Benaglia,[34] and Seidel,[19] have

addressed crucial catalyst, *in-situ* formed, design parameters including operational stability and partially saturated coordination environment. In general, the designed ligands provide two or three heteroatoms for coordination. Our group has recently initiated a project aimed at developing efficient methodologies to promote the A^3 coupling using Cu(II) coordination compounds.[35] From these initial studies, the optimum pre-catalyst features a Cu(II) center with octahedral $\{N_4O_2\}$ geometry and the, retained in solution, planar $\{N_4\}$ geometry of Cu(II) is a crucial factor that a favours the coordination of the alkyne with concomitant activation of the C–H bond and the formation of the corresponding Cu(I)-acetylide.

Salen[36] ligands offer a $\{N_2O_2\}$ planar coordination pocket. Stack demonstrated the peculiar redox potential of Cu-salen compounds in different oxidation states revealing the non-innocent character of the salen based ligands.[37–39] Depending on various parameters (i.e. ligand substitution, temperature, solvent) oxidation or reduction can occur at the ligand or the metal centre of these species,[40,41] followed by C–C bond activation across two monomeric units and thus yielding infinite components via radical pathways.[42–46] Moreover, in Cu-salen derivatives reversible methanolysis of an azomethine C=N bond can be observed.[47] Bearing all these in mind, we envisaged that a well-characterised Cu(II)-salen derivative would be an efficient vehicle towards the A^3 coupling; recent works support this hypothesis,[48,49] although evidence of the mechanism is uncertain. Inspired by our recent work with salen based ligands,[50] we identified that a Cu(II)-salen compound made with the ligand (H_2L) shown in Scheme 1 is an ideal candidate to serve this purpose.[51] The substitutions on the ligand have a twofold role; to promote the reduction of the metallic centre from Cu(II) to Cu(I) through radical pathways, even at room temperature and under non-inert atmospheric conditions,[37–46] and simultaneously prevent self-polymerisation via C-C bond activation. To the best of our knowledge and our surprise, this is the first crystallographic report of the enantiomerically pure {Cu(II)L} (**1S**) component shown in Scheme 1.[52,53] Moreover, control experiments, SXRD, cyclic

voltammetry and theoretical studies shed light on the mechanism of this reaction. The scope and limitations of this methodology are also discussed.

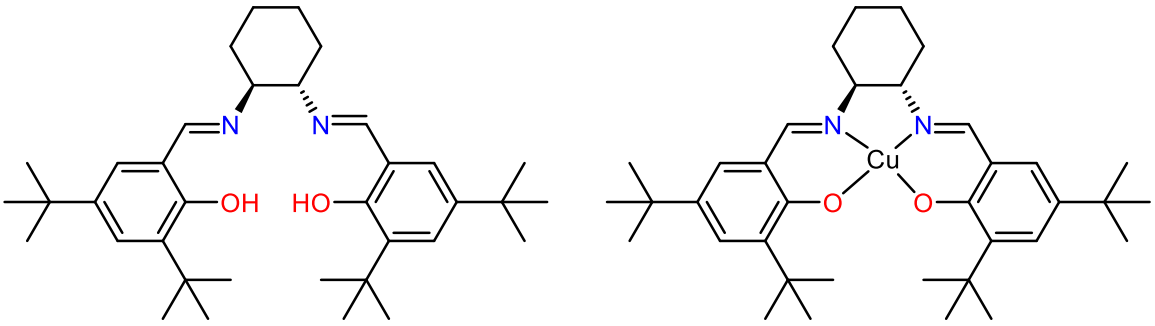

Scheme 1. The chosen ligand (left) and the enantiomeric pure Cu(II) catalyst (**1S**) used in this study (right).

Results and Discussion

The enantiomerically pure version of the ligand (H_2L^S) can be synthesised in one high yielding step (yields over 95%) by refluxing the corresponding (1S,2S)-(−)-1,2-Diaminocyclohexane and 3,5-di-*tert*-butyl-2-hydroxybenzaldehyde in EtOH. Then, the combination in open air of H_2L^S with $Cu(OTf)_2$ $2H_2O$, at room temperature and under ambient conditions, in the presence of Et_3N in MeOH, in a molar ratio 1:1:2, afforded the air-stable compound [Cu(II)L^S] (**1S**) in yields over 80%; noteworthy the total yield for the synthesis of the catalyst is 76%. Reactions of H_2L^S with other Cu(II) salts, $CuCl_2$, $Cu(NO_3)_2$ $3(H_2O)$, $CuBr_2$, $Cu(ClO_4)_2$ $6(H_2O)$ in the presence of a base, yield **1S**, but lower yields (<65%). The enantiomeric compound was obtained as brown crystals and characterised by SXRD (Figure 1), IR, UV-Vis, Circular Dichroism (CD), Elemental analysis, Thermogravimetric analysis (TGA) and Electron Spray Ionization Mass Spectroscopy (ESI-MS). The Cu centre is coordinated by the salen ligand, resulting in a distorted square-planar geometry (Figure 1) and there are two independent moieties in the asymmetric unit. The distance between the two Cu(II) adjacent centres is 5.094Å, while weak C-H···aryl but no aromatic interactions can be identified. The Cu – O and Cu – N bond distances are typical for a Cu(II) compound and following previous crystallographic characterised components (see Table S1).[37,42,52,54] Both compounds show one

peak in the ESI-MS (positive-ion mode) at m/z 607.9719 which perfectly corresponds to the fragment, in MeOH, i-PrOH and DCM solvents (Figures S3), indicating that the structure remains intact in these solvents. Circular Dichroism studies of **1S** in MeOH and DCM solvents in a concentration 0.3M confirm the chiral nature of the complex (Figures S4&S5). Thermogravimetric analysis of **1S**, under N_2 atmosphere, shows that the material is stable up to 288^{o}C, and then decomposition starts; the final residue corresponds to CuO (exp 13.07%, found 12.08%) (Figure S6). The UV-Vis spectra of **1S** in DCM solvent is typical of a Cu(II) chromophore with $\{N_2O_2\}$ environments, respectively, at various concentrations (Figure S7).[55,56]

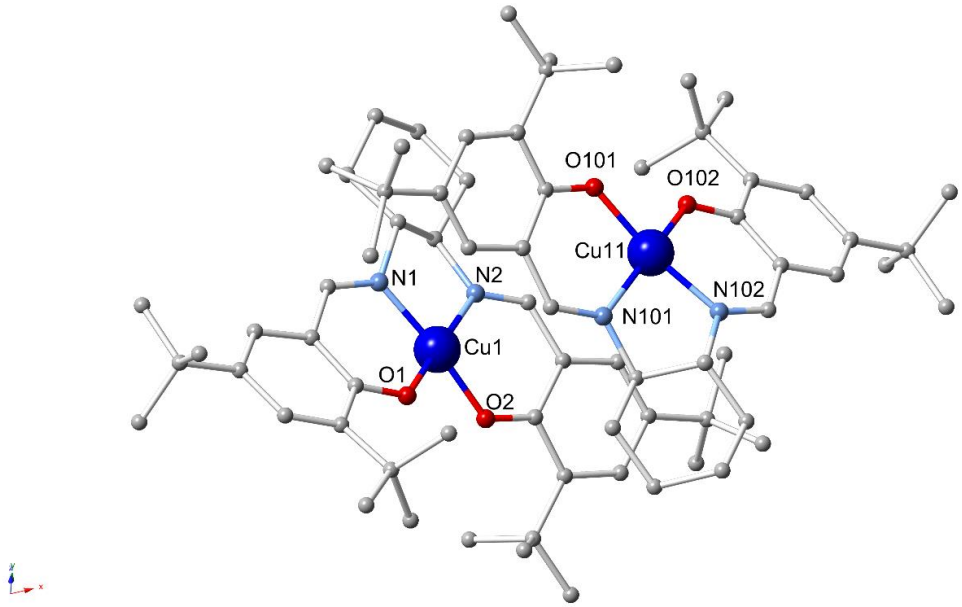

Figure 1. A projection of the asymmetric unit of **1S.**

With the catalyst in hand and aiming to develop a user-friendly protocol, we performed reactions in the open air and considered that **1S** would be an ideal candidate for aliphatic aldehydes and secondary amines. Cyclohexanecarboxaldehyde, pyrrolidine, and phenylacetylene were chosen as model substrates to evaluate the title reaction in a molar ratio 1: 1.1: 1.2 (Table 1). Given that the starting component consists of Cu(II), prolonged reactions were performed to allow reaction completeness and different solvents were used. Reactions

with polar and coordinating solvents such as MeOH and EtOH (Entries 1 and 2, Table 1) gave low yields; however, the reactions in i-PrOH gave **5aaa** in a moderate yield; this outcome is in line with our previous findings.[35] The reactions in CH_3CN and DCM (Entries 4&5, Table 1), had a better performance, while reactions in other solvents (Entries 6-10, Table 1) gave **5aaa** in traces. The use of molecular sieves (Entry 11, Table 1) in DCM increases the yield of the final product. Reactions with coordinating solvents lower the catalytic efficacy; this behaviour may be explained by solvent coordination to the metal centre, which prohibits substrate binding. This finding is in line with other experiments with and without the presence of molecular sieves; the latter captures the released H_2O byproduct which may coordinate to the Cu centre, thus giving the expected product in higher yield.

Table 1. Solvent screening

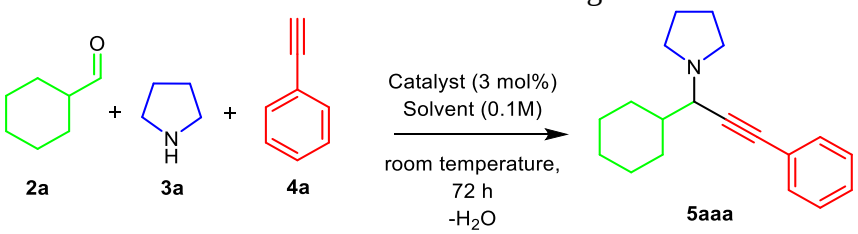

Entry	Solvent	Yield (%)[a,b]
1	MeOH	16
2	EtOH	22
3	i-PrOH	64
4	CH_3CN	74
5	DCM	71
6	Acetone	No reaction
7	$CHCl_3$	traces
8	Toluene	traces
9	Hexane	11
10	Ethyl acetate	No reaction
11	**DCM**	**74[c]**
12	-	95

[a]Relative yield calculated by ^{1}H-NMR based on the remaining **2a**;[b]Reaction conditions, catalyst (3 mol%), 1.0 mmol aldehyde, 1.1 mmol amine, 1.2 mmol alkyne, catalyst (3%), 5mL solvent, 72 hours, room temperature, Concentration 0.1M; [c] In the presence of molecular sieves 4Å

Interestingly, a reaction in the absence of solvent (Entry 12, Table 1),[57] gave **5aaa** in 95%, however, to avoid unexpected solidification of the final products and to take all the above notes,

we chose DCM as the solvent for the subsequent reactions and the use of molecular sieves to capture by-product H_2O molecules.

A control experiment in the absence of any catalyst, under the above-identified conditions, failed to produce product **5aaa**. To further evaluate the catalytic efficacy of compound **1S**, we extended the pilot experiments varying concentration, loading, reaction time and other parameters. Concentration experiments (Entries 1-3, Table 2) identify that the reaction is highly dependent, and the optimum performance is obtained in a reaction with 0.4M (1mmol in 2.5ml). Keeping the concentration to 0.4M, the catalyst' loading experiments (Entries 4-6, Table 2) identify that a 2 mol% is ideal, while shorter reactions (Entries 7-8, Table 2) gave **5aaa** in lower yields. A reaction at a higher temperature and shorter time (Entry 9, Table 2) gave **5aaa** in good yield.

Table 2. Optimisation of Reaction Conditions

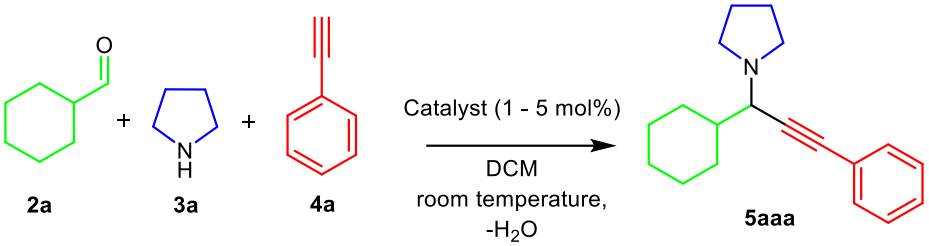

Entry	Loading (mol %)	Time (h)	Yield (%)[a,b]
1	3	72	75[c]
2	3	72	84[d]
3	3	72	96[e]
4	**2**	**72**	**97[e]**
5	1	72	93[e]
6	5	72	87[e]
7	2	24	43[e]
8	2	48	86[e]
9	2	24	88[e,g]
10	**2**	**0.5**	**>99[h]**

[a]Relative yield calculated by ^{1}H-NMR based on the remaining **2a**, [b]Reaction conditions 1.0 mmol aldehyde, 1.1 mmol amine, 1.2 mmol alkyne, molecular sieves, solvent DCM, room temperature, [c]Concentration 0.2M. [d]Concentration 0.3M, [e]Concentration 0.4M [g] 50°C, [h]Microwave conditions 80°C, 30 min.

The optimised protocol (2 mol% loading, room temperature, 72 hours, after that named as Methodology **A**) is appealing since it operates in the absence of base and additives and at room temperature, however, to overcome the increased reaction time, we considered using the microwave approach to increase the reaction rates. Following the above protocol, all the reactions were performed in a microwave at low temperature (80^{o}C), catalyst loading (2 mol%), in the open air and were complete within 30 minutes see Table 2, entry 10 (named after that as Methodology **B**). Methodology **B** is far more efficient when compared with other reported Cu based microwave protocols that yield propargylamines. These methods require Ar atmosphere high catalyst loading (15 mol%) and temperatures above 100^{o}C.[58] The next step was to identify the limitations of both methodologies, and therefore we extended the scope of the reaction (Table 3) by employing a variety of secondary amines, aliphatic aldehydes and alkynes and produce in total twenty propargylamines out of which nine scaffolds are new. In all cases, the reaction proceeded smoothly, and we were able to isolate the corresponding products in good to excellent yields. For compound **5caa**, following already known chiral column HPLC protocols,[19] we identified a (75/25) 50 % ee for the product resulting with methodology **A**. This low level of enantioselectivity has been observed in other systems,[34] without significant improvement, whilst the elevated temperature in methodology **B** removes the enantioselective character of the system, therefore we decided to discard the enantioselective characterisation of the remaining products. For compound **5fda**, the NMR data showed the presence of two diastereoisomers with a ratio of 57:43 and 55:45, for methodology **A** and **B**, respectively.

Table 3. Scope of the reaction with aldehydes, secondary amines and alkynes.[a,b]

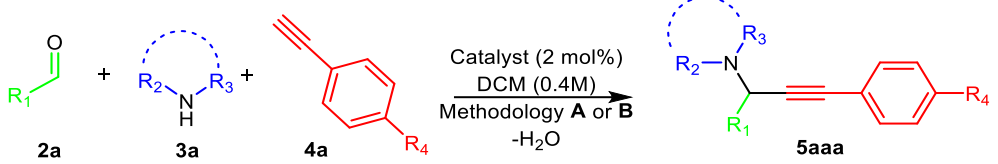

2a 3a 4a 5aaa

5aaa
A. 97%
B. >99%

5aba
A. 98%
B. >99%

5aca
A. 93%
B. 95%

5ada
A. 96%
B. >99%

5baa
A. 79%
B. 79%

5bca - NEW
A. 79%
B. 90%

5bda - NEW
A. 94%
B. >99%

5bea-NEW
A. 91%
B. 96%

5caa
A. 83%
B. 87%

5daa
A. 80%
B. 85%

5dba
A. 69%
B. 78%

5dca-NEW
A. 66%
B. 70%

5eaa
A. 19%
B. 31% (55%)[c]

5eca-NEW
A. 16%
B. 30% (53%)[c]

5aab
A. 97%
B. 97%

5fda-NEW
A. 71% dr(43%)
B. 85% dr(57%)

5adb - NEW
A. 95%
B. >99%

5bab - NEW
A. 79%
B. 84%

5bdb-NEW
A. 90%
B. 93%

5afa
A. 73%
B. 88%

[a]Isolated Yields, [b]Reaction conditions, catalyst (2 mol%), 1.0 mmol aldehyde, 1.1 mmol amine, 1.2 mmol alkyne, molecular sieves, solvent DCM, concentration 0.4M, Methodology **A** (72 hours, room temperature), Methodology **B** (MW, 80ºC, 30min).[c] MW, 80ºC, 1h.

To further validate the suitability of **1S** for the A^3 coupling, we performed control experiments using aniline (primary instead of secondary amine), benzaldehyde and phenylacetylene. The reason for this selection is that this reaction produces an oxonium H_3O^+ entity as a temporary byproduct (1 H_2O molecule from the Schiff base and the abstracted proton from the triple bond), instead of water. After 72 hours, the expected product is produced in low yield (35%), indicating that modification of the catalytic system is required for **1S** to be suitable for primary amines.

Reactivity - Mechanistic studies. Aiming to investigate the role of **1S** in the reaction and shed light on the reaction mechanism, we performed a series of experiments altering reaction parameters following methodology **A**. Notably, reactions under N_2 (Entry 1, Table 4) or Ar (Entry 2, Table 4) atmosphere gave **5aaa** in 97 and 95%, respectively. These data disfavour the incorporation of O_2 in the present catalytic cycle, that means the possible formation of the dimeric intermediate Cu-O_2-Cu with variable oxidation states; the latter has been identified as a critical factor in other C-C activation reactions catalysed by Cu(II) components.[59–61] Moreover, the addition of 10 mol% TEMPO (Entry 3, Table 4) under these conditions had a significant impact leading to activity cessation. This result signifies the presence of a radical pathway containing the Cu(I)-complex species and supports the plausible *in-situ* formation of the Cu(I)-acetylide intermediate, that may be responsible for the catalytic cycle.

Then we performed an experiment with *in-situ* preparation of the catalyst (Entry 4, Table 4). The one-pot reaction containing H_2L^S and the weakly binding metal salt $Cu(OTf)_2$ yielded **5aaa** in 96%. This data is indeed an impressive result, in line with other reported similar studies,[62] however, it is unclear if the formation of the neutral complex **1S** proceeds before catalysis and/or the metal salt promotes the organic transformation. In terms of operation ability, we believe that this in-situ protocol is weak because of the following three factors. A) Two protons are released from the parent organic ligand upon complexation; these may

participate in the organic transformation by facilitating the formation of H_2O byproduct molecules. B) The triflate is an extremely stable anion, the conjugate base of a very strong acid; therefore it may abstract a proton, forming triflic acid which in turn may facilitate the redox Cu(II)-Cu(I) converse. C) A reaction using solely $Cu(OTf)_2$ as the catalyst, under similar conditions (Entry 5, Table 4) provides **5aaa** almost quantitatively while reactions with other Cu(II) salts discard the formation of **5aaa**. These results showcase that the hydroxide (OH^-) moiety, produced from the condensation of aldehyde and secondary amine, is not an efficient base to facilitate acetylenic proton abstraction and/or the redox Cu(II)-Cu(I) converse, therefore the combinatorial, or not, role of the two different bases (OH^- and ^-OTf) and the role of $Cu(OTf)_2$ in this A^3 catalytic cycle are questioned. We decided to investigate this protocol in future experiments.

Table 4. Various experiments to obtain mechanistic evidences.

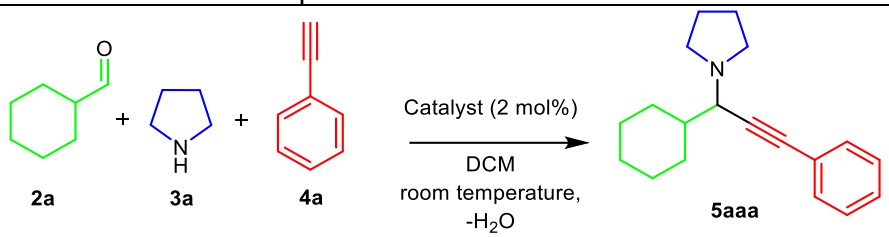

Entry	Time (h)	Atmosphere	Additives	Yield (%)[a,b]
1	72	N_2	-	97
2	72	Ar	-	95
3	72	open- air	TEMPO (10 mol%)	0
4	72	open-air	-	96[c]
5	72	open-air	-	100[d]
6	72	open-air	-	96[e]
7	72	open-air	-	95[f]
8	72	open-air	-	95[g]
9	72	open-air	-	94[h]

[a]Relative yield calculated by ^{1}H-NMR based on the remaining **2a**, [b]Reaction conditions, catalyst (2 mol%), 1.0 mmol aldehyde, 1.1 mmol amine, 1.2 mmol alkyne, molecular sieves, solvent DCM 2.5mL, concentration 0.4M, room temperature. [c]In-situ formation of the catalyst $H_2L/Cu(OTf)_2$ H_2O.[d] $Cu(OTf)_2$ [e]Recovered (1 cycle) catalyst [f]Recovered (2 cycles) catalyst. [g]Recovered (3 cycles) catalyst. [h]Recovered (5 cycles) catalyst

To identify the potential of our catalytic system, we attempted to recover the catalyst. After reaction completion, the crude product was placed in the fridge or left unattended in the

open air, and well-formed needle-like brownish coloured crystals grew within two hours or four days, respectively. The recovered material was tested and found to catalyse the reaction without loss of its activity (Entries 6- 9, Table 4); the procedure was repeated five times, without observing a loss of the catalytic efficacy. To further shed light on this performance, we attempted SXRD characterisation of the recovered material **1S'** (after one cycle). The crystal used for the structure determination of **1S'** was twinned. Despite obtaining almost identical unit cell parameters, slight differences in bond distances could be identified. (Table 5). These were mainly associated to only one of the two independent entities in the asymmetric unit and the three main differences prior and post catalysis, respectively, are a) an imine C=N bond 1.255(13)Å and 1.284(10)Å, b) one Cu-N bond 1.916(8)Å and 1.940(6)Å, c) one Cu-O bond 1.893(7) Å and 1.910(5)Å. Interestingly, significant changes in the C–C bonds in both aromatic rings can be observed (Table S2). Moreover, Bond Valence Sum analysis[63] (Table S3) for **1S** prior and post catalysis signifies a slight (~3 %) change in the oxidation state of the Cu centre. The crystallographic datasets for **1S** and **1S'** were collected in different instruments (see ESI) but at the same temperature (100K). To validate these differences, we collected a further three crystallographic datasets for each catalyst, **1S** and **1S'** at the same temperature (100K) and using the same diffractometer. The data (Tables S4) indicate that there are only minor variations in bond lengths and unit cell parameters between **1S** and **1S'** and therefore exclude the possibility of structural change/alteration of the oxidation state of the metal centre in the recovered catalyst. In these six different data, the Cu – O and Cu – N bonds vary from 1.869 Å to 1.914 Å and from 1.911 Å to 1.939 Å, respectively, whilst more considerable differences can be found in only one sample for the C=N bonds (1.250(13) Å, 1.288(14) Å and 1.291(13) Å, 1.325(13)Å) but this crystal was twinned and of low quality. A crystallographic dataset was collected for the recovered catalyst after the 5th run, which confirmed that stability and integrity

of the system. Moreover, the UV-Vis spectrum (in DCM) and TGA analysis of **1S'** showed similar behaviour to that of **1S** (Figures S8&9).

Table 5. A ChemDraw diagram listing the significant structural difference in bond lengths between initial and recovered catalyst

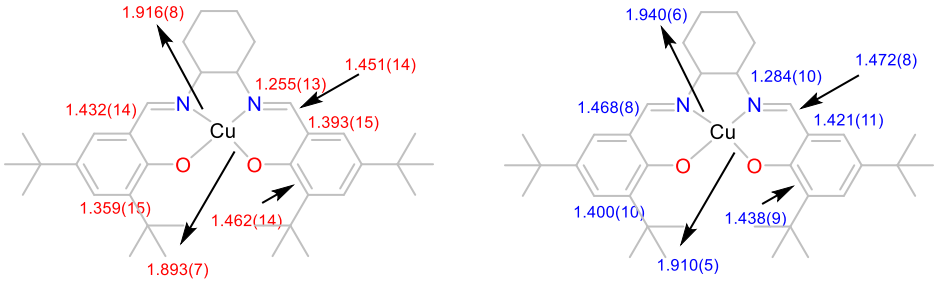

Crystal Data	1S	1S'
a(Å)	9.8740(4)	**9.8853(2)**
b(Å)	13.5904(5)	13.5954(3)
c(Å)	14.8719(6)	14.8780(2)
α(°)	62.868(4)	62.868(2)
β(°)	73.368(3)	73.374(2)
γ(°)	78.772(3)	**78.798(2)**
V(Å^3)	1696.94(13)	**1700.32(7)**
T/K	100(2)	100(2)
Bond distances and angles with significant differences		
N=C	1.255(13)	**1.284(10)**
Cu-N	1.916(8)	**1.940(6)**
Cu-O	1.893(7)	**1.910(5)**

To further shed light on the mechanism of this reaction the electrochemical behaviour of the ligand, **1S**, **1S'** and titrations of **1S** or **1S'** with phenylacetylene (Ph-C≡C-H) were studied in CH_2Cl_2 by cyclic voltammetry under N_2. The ligand exhibits two distinct quasi-reversible waves (Figure S10) that correspond to two successive oxidations of a phenol into a phenoxyl radical.[38,64] The cyclic voltammograms of **1S** display two well-separated one-electron reversible redox waves at $E_{1/2}^1$ = 0.51 and $E_{1/2}^2$ = 0.81 V V vs Fc^+/Fc for **1S** and $E_{1/2}^1$ = 0.52V and $E_{1/2}^2$ = 0.81 V for **1S'** which showcase a typical behaviour with the reported similar systems (Figure S11).[38,64,65] In the reductive region (Figure 2), **1S** and **1S'** both show a non-reversible

reduction. Notably, when a fresh sample of **1S** and a sample of **1S'** were titrated with Ph-C≡C-H (0, 0.5, 1, 2, and 50 equivalent for **1S** and 0, 0.5, and 50 for **1S'**, 50 equivalents correspond to 2% catalyst loading), no significant effects on the oxidative process were observed. However, both **1S** and **1S'** show slightly different cathodic behaviour in the presence of Ph-C≡C-H. The cathodic wave's current slightly increases with the concentration of Ph-C≡C-H, and a new feature appears during the back scan. This different behaviour may be attributed to the reduction of the [Cu(II)/Ph-C≡C-H] species to the [Cu(I)/Ph-C≡C-H] species as this notion has been well established in other protocols.[66,67] To further establish this notion, UV-Vis titration studies at room temperature and in the open air of **1S** and **1S'** and Ph-C≡C-H in a catalytic ratio (2:100) were performed (Figures S8-S9), with no noted differentiation.

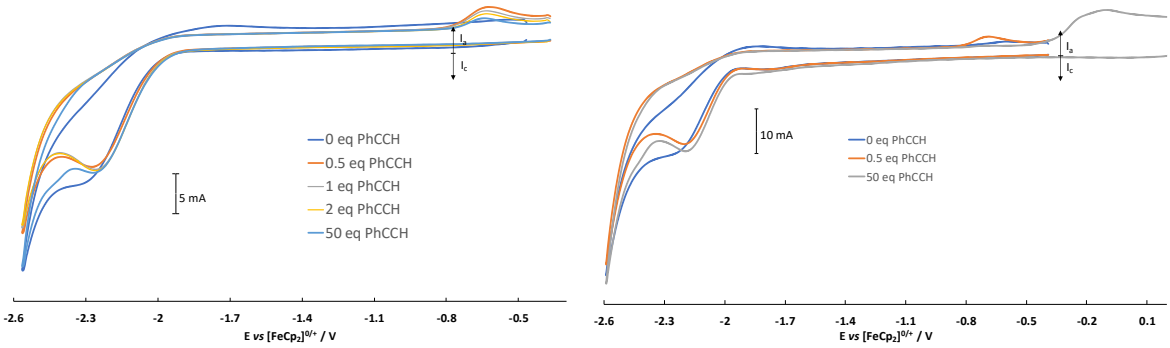

Figure 2 CV data in the reductive region of **1S** (left) and **1S'** (right) in the presence of phenylacetylene.

It is worth noting that in the crude NMR spectra of all the above-studied reactions, no parent organic ligand nor the formation of the hetero coupling (bis-adduct) product of terminal alkynes were observed, whereas precipitation of metallic Cu was not observed. Bearing in mind that a) terminal alkynes can reduce Cu(II) to Cu(I),[66,67] b) proton abstraction from the catalyst has been noted in mononuclear systems,[68] c) the reaction takes place in a non-coordinating solvent, in the absence of base and at room temperature and d) the reaction rates and efficacy increase with temperature or microwaves, we propose the following three-step mechanism.

Initially, the planar {N_2O_2} geometry of Cu(II) promotes alkyne binding with concomitant activation of the C–H bond. In step II, the acetylenic proton is abstracted from one nitrogen atom of the organic framework to form the corresponding Cu-acetylide, which may be stabilised by radical pathways. This notion has been recently proposed in a similar system.[69] Then, the symmetrical {N_2O_2} plane accounts for adequate electron delocalisation to ensure the reduction of Cu(II) to Cu(I) which then orchestrates the breaking of the Cu-O bond as well as positional rearrangement of the acetylide group. Finally, the addition of the Cu(I)-acetylide to the *in-situ* generated iminium ion yields the corresponding propargylamine derivative and water, and regeneration of the catalyst. Given the absence of an initiator and that the reduction of Cu(II) to Cu(I) can be prolonged,[70] we may envisage that step II is the rate-determining step. It is well known in synthetic chemistry,[71,72] especially for radical-triggered cascade reactions,[73] that the Cu(I)-acetylide intermediate can be formed by a Single Electron Transfer (SET) mechanism, therefore the proposed mechanism (Scheme 2) accounts all parameters (oxidation states, proton abstraction, by-product formation, substrate-coordination, metal coordination geometry) and we believe that is highly likely for the mechanism to follow a SET pathway.

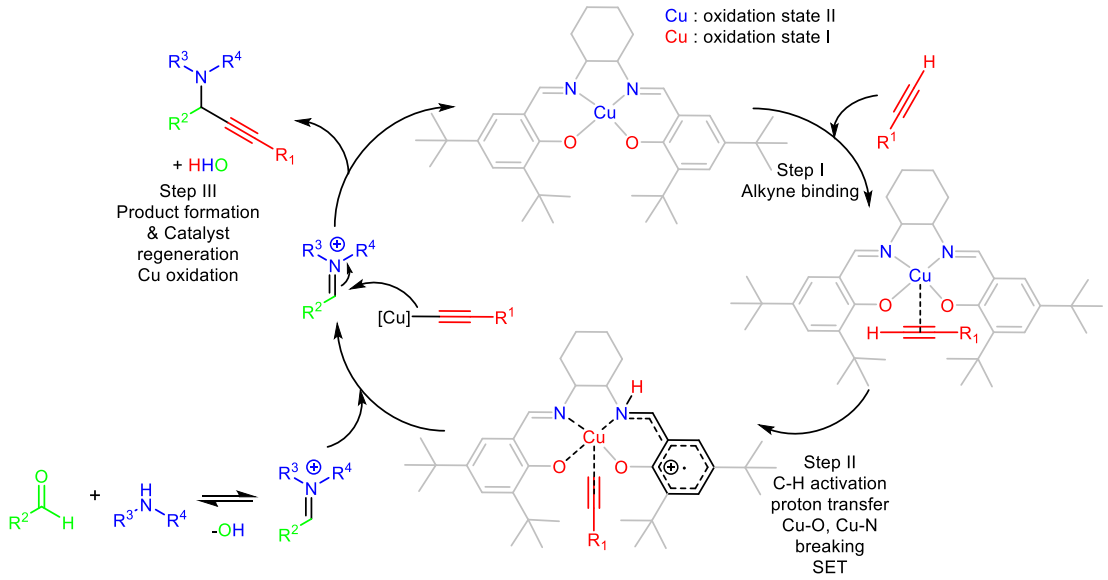

Scheme 2. A plausible mechanism for this reaction.

To further validate this notion, we synthesised the racemic reduced version of the organic ligand and the corresponding Cu(II)-salan compound (**6**) (Scheme 3, Figure S12), following an already known synthetic protocol.[54] The reduced organic scaffold provides a similar coordination environment to the metal centre and may generate *in-situ* radicals due to the presence of the phenoxide moieties. Notably, in previous results, compound **6** was found to perform poorly in oxidation and oxidative coupling reactions, when compared to the corresponding derivative of **1S**.[54] A reaction with **6** as the catalyst under similar reaction conditions (Scheme 3) yields **5aaa** in a very good yield, similar to that of **1S**, supporting our reasoning for topological control which permits alkyne binding with concomitant activation of the C–H bond and simultaneous accommodation of the abstracted acetylenic proton, and continuous generation, via *in-situ* generated radicals, of a transient Cu(I) active site.

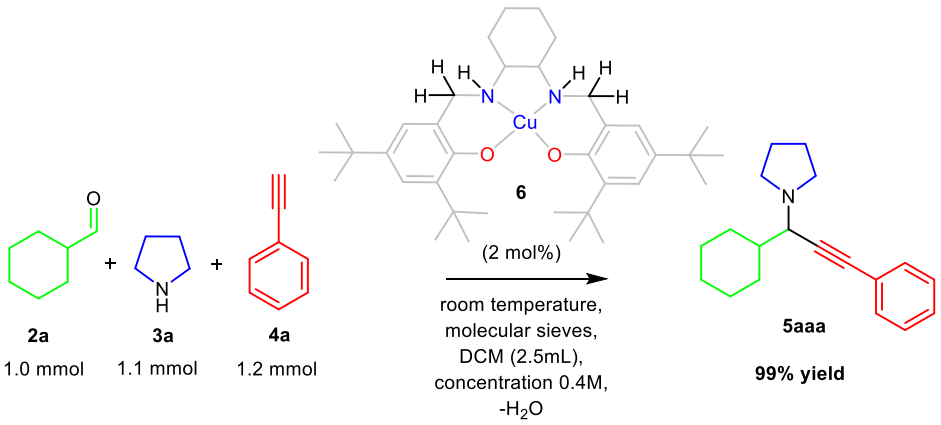

Scheme 3. The pilot reaction that the racemic Cu(II)-salan compound (**6**) was tested as a catalyst.

Mechanistic studies employing DFT computational protocols. To further understand the mechanism of the A^3 coupling reactions catalysed by **1S**, we performed density functional theory (DFT) calculations to model the geometric and energetic reaction profile. All the DFT calculations throughout this work were carried out using the Gaussian09 software package.[74] The geometries and thermal corrections for all stationary points along the reaction coordinate

are computed with the Perdew, Burke and Ernzerhof[75-81] of hybrid density functional denoted as PBE0 (also called PBE1PBE) as implemented in the Gaussian09 program suite. For the geometry optimisations, we have used the Def2-TZVP basis set.[82,83] Hereafter the method used in DFT calculations is abbreviated as PBE0/Def2-TZVP. Frequency calculations were also performed at the same level of theory to identify whether the stationary point is a local minimum or a transition state. The natural bond orbital (NBO) population analysis was performed using Weinhold's methodology as implemented in the NBO 6.0 software.[84-86]All calculations were performed in solution (CH_3OH solvent) employing the Polarizable Continuum Model (PCM) using the integral equation formalism variant (IEFPCM) being the default self-consistent reaction field (SCRF) method.[87]

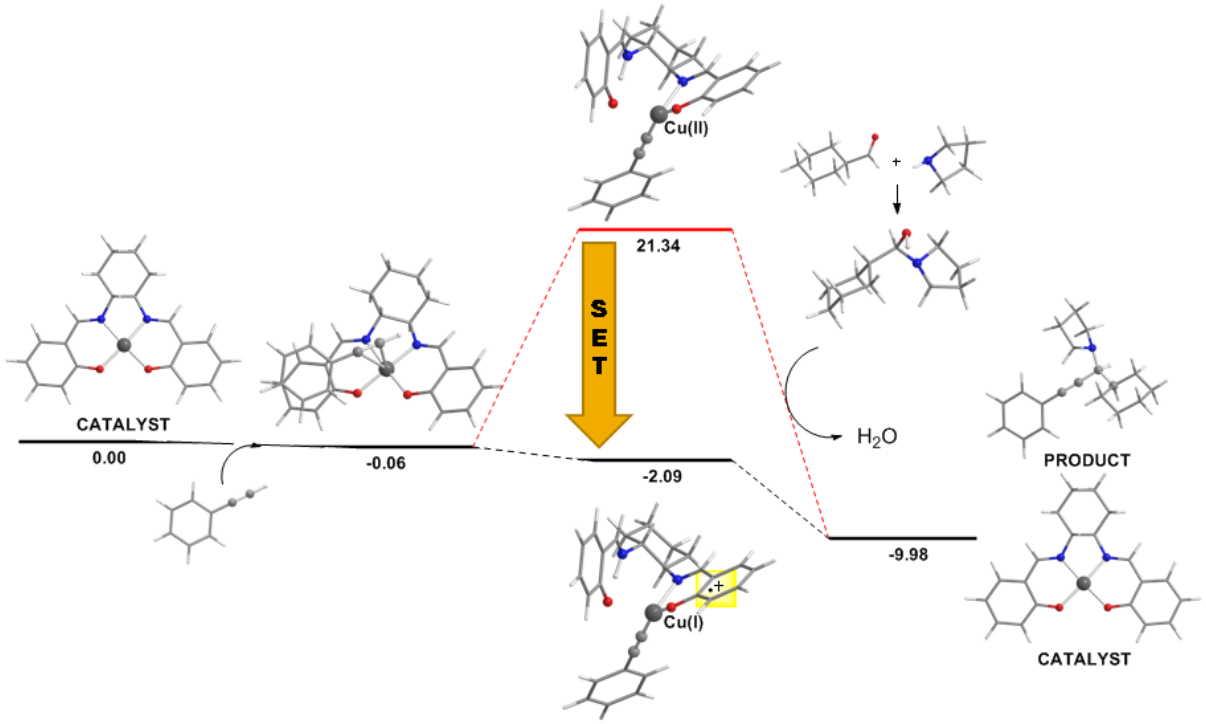

Figure 3. Geometric and energetic (ΔH in kcal/mol) reaction profile for the A^3 coupling reactions catalysed by **1S** calculated at the PBE0/Def2-TZVP level of theory in a solution using methanol solvent.

The geometric and energetic reaction profile calculated at the PBE0/Def2-TZVP level of theory in solution (CH_3OH solvent) is depicted schematically in Figure 3, while the geometrical structures of all reactants, intermediates and products directly optimised in solution phase are given in the SI (Figure S14). It is important to note that the optimised geometry of the catalyst in methanol solution (Figure S14) matches better to the crystal structure of the recovered **1S'** and not the initial **1S** catalyst.

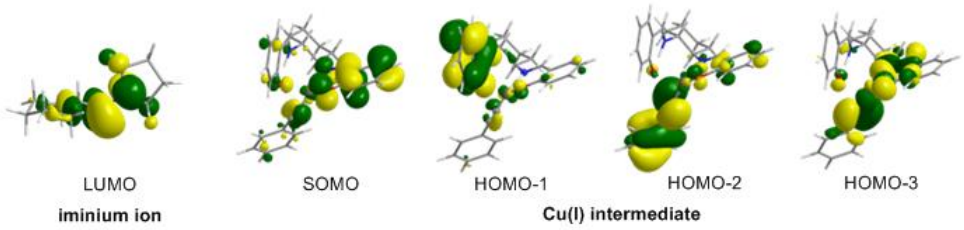

Scheme 4. Frontier Molecular Orbitals (FMOs) of the iminium ion and the Cu(I) intermediate.

The course of the reaction involves initially a loose association of Ph-C≡C-H to Cu(salen) complex in an orientation almost parallel to the coordination plane with the H atom directed towards an N donor atom of the salen ligand. The estimated interaction energy in the adduct formed is only 0.06 kcal/mol. This orientation of Ph-C≡C-H activates the C-H bond of Ph-C≡C-H accompanied by the proton transfer to the N-donor atom of the coordinated salen ligand and coordination of the phenylacetylide ligand to Cu(II) centre in a η^1-mode. The proton detachment process demands 213.4 kcal/mol with the proton affinity of the N-donor atom of salen estimated to be 144.8 kcal/mol. The proton transfer also promotes the rupture of one of the Cu-O bonds yielding a three-coordinated Cu(II) complex (Figure S14). The three-coordinated Cu(II) intermediate concomitantly is reduced to a three-coordinated Cu(I) intermediate by intramolecular single electron transfer (SET) from the Single Occupied Molecular Orbital (SOMO) localized mainly on the coordinated phenoxo moiety of the protonated salen ligand towards the Highest Occupied Molecular Orbital (HOMO) exhibiting high 3*d* character (*cf* HOMO-3, Scheme 4). The intramolecular Cu(II) → Cu(I) reduction stabilises the three-coordinated Cu(I) intermediate by 23.43 kcal/mol concerning the Cu(II)

congener considering an adiabatic SET. Notice that the experimentally determined reduction potential for **1S** is 1.02 V (23.52 kcal/mol). Next, the Cu(I)-intermediate having an open coordination sphere dispose of open channels for the *in-situ* generated electrophilic iminium ion to attack the nucleophilic C atom of the coordinated phenylacetylide, thus affording the corresponding propargylamine product and water and regenerating the catalyst. The condensation of the cyclohexanecarboxaldehyde with pyrrolidine affording the cyclohexyl(pyrrolidin-1-yl)methanol aldol is exothermic (ΔH = -4.86 kcal/mol), while the generation of the iminium ion by the detachment of the hydroxyl group from the aldol demands 45.79 kcal/mol. Notice that the electrophilic C atom of the iminium ion and the nucleophilic C atom of the coordinated phenylacetylide acquire natural atomic charges of 0.318 |e| and -0.375 |e| respectively. An inspection of the Frontier Molecular Orbitals (FMOs) of the iminium ion and the Cu(I) intermediate (Scheme 4) reveals that the formation of the propargylamine product is also supported by LUMO (iminium) – HOMO-2 (Cu(I) intermediate) interactions.

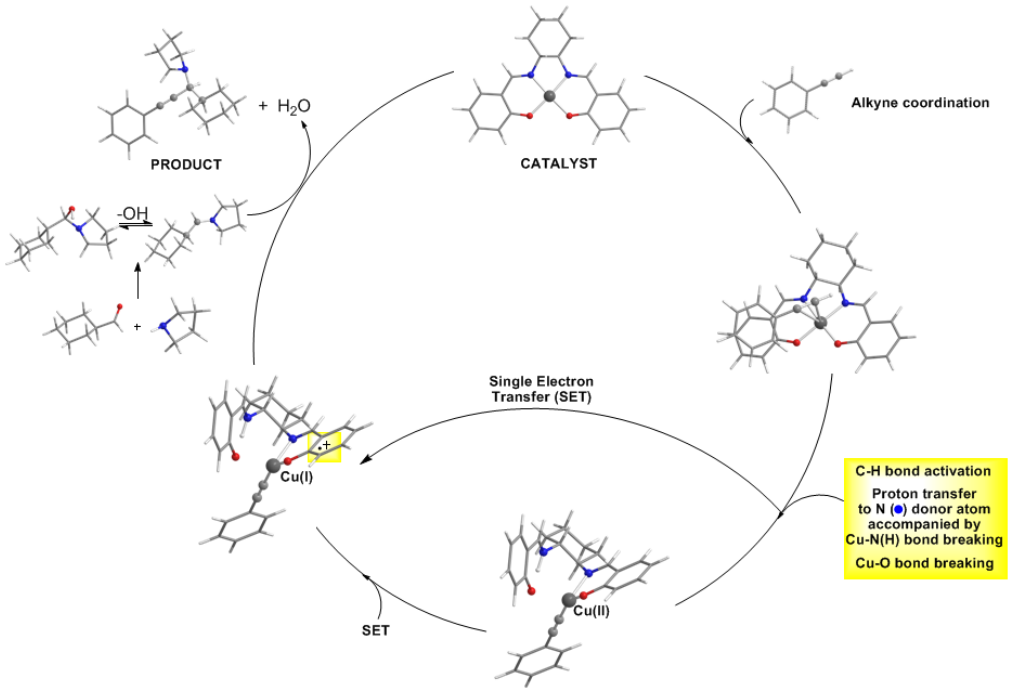

Scheme 5. The proposed reaction mechanism for the A^3 coupling reactions catalysed by **1S** calculated at the PBE0/Def2-TZVP level of theory in methanol solution.

In summary, the full catalytic cycle, supported by DFT calculations, is shown in Scheme 5, which is consistent with the proposed plausible catalytic cycle supported by experimental measurements.

Conclusions

We present a Cu(II) based protocol that efficiently catalyses the A^3 coupling reaction in the open air and at room temperature. Vital to the success of this is the use of the phenoxido salen-based ligand which orchestrates topological control permitting alkyne binding with concomitant activation of the C–H bond and simultaneously acting as template temporarily accommodating the abstracted acetylenic proton, and continuous generating, via in-situ formed radicals and Single Electron Transfer (SET) mechanism, of a transient Cu(I) active site to facilitate this transformation. The present study identifies first-principle structural features for this well-characterised Cu(II) system in the open air and paved the way for the future development of this easy to make and handle system that may apply to several organic transformations and asymmetric synthesis.

Acknowledgements

GEK thanks Dr. Ioannis Lykakis for fruitful discussions and the EPSRC UK National Crystallography Service at the University of Southampton for the collection of the crystallographic data for **1S** and **1S'**.[88]

References

1 A. Dömling, W. Wang and K. Wang, *Chem. Rev.*, 2012, **112**, 3083–3135.

2 K. Lauder, A. Toscani, N. Scalacci and D. Castagnolo, *Chem. Rev.*, 2017, **117**, 14091–14200.

3 I. Jesin and G. C. Nandi, *Eur. J. Org. Chem.*, 2019, 2704–2720.

4 V. A. Peshkov, O. P. Pereshivko and E. V. Van der Eycken, *Chem. Soc. Rev.*, 2012, **41**, 3790–3807.

5 B. V. Rokade, J. Barker and P. J. Guiry, *Chem. Soc. Rev.*, 2019, **48**, 4766–4790.

6 B. V. Rokade and P. J. Guiry, *J. Org. Chem.*, 2019, **84**, 5763–5772.

7 S. Layek, B. Agrahari, S. Kumari, Anuradha and D. D. Pathak, *Catal. Letters*, 2018, **148**, 2675–2682.

8 W. Fan, W. Yuan and S. Ma, *Nat. Commun.*, 2014, **5**, 1472–1483.

9 P. H. S. Paioti, K. A. Abboud and A. Aponick, *J. Am. Chem. Soc.*, 2016, **138**, 2150–2153.

10 T. Sugiishi, A. Kimura and H. Nakamura, *J. Am. Chem. Soc.*, 2010, **132**, 5332–5333.

11 X. Zhang and A. Corma, *Angew. Chemie - Int. Ed.*, 2008, **47**, 4358–4361.

12 B. Karimi, M. Gholinejad and M. Khorasani, *Chem. Commun.*, 2012, **48**, 8961–8963.

13 C. Wei and C.-J. Li, *J. Am. Chem. Soc.*, 2003, **125**, 9584–9585.

14 V. K.-Y. Lo, C.-Y. Zhou, M.-K. Wong and C.-M. Che, *Chem. Commun.*, 2010, **46**, 213–215.

15 C. Wei, Z. Li and C.-J. Li, *Org. Lett.*, 2003, **5**, 4473–4475.

16 Y. Zhao, X. Zhou, T.-A. Okamura, M. Chen, Y. Lu, W.-Y. Sun and J.-Q. Yu, *Dalton Trans.*, 2012, **41**, 5889–5896.

17 N. Salam, A. Sinha, A. S. Roy, P. Mondal, N. R. Jana and S. M. Islam, *RSC Adv.*, 2014, **4**, 10001–10012.

18 N. Sharma, U. K. Sharma, N. M. Mishra and E. V Van Der Eycken, *Adv. Synth. Catal.*, 2014, **356**, 1029–1037.

19 C. Zhao and D. Seidel, *J. Am. Chem. Soc.*, 2015, **137**, 4650–4653.

20 L. Shi, Y.-Q. Tu, M. Wang, F.-M. Zhang and C.-A. Fan, *Org. Lett.*, 2004, **6**, 1001–1003.

21 T. T. T. Trang, D. S. Ermolat'ev and E. V. Van der Eycken, *RSC Adv.*, 2015, **5**, 28921–28924.

22 H.-B. Chen, Y. Zhao and Y. Liao, *RSC Adv.*, 2015, **5**, 37737–37741.

23 L. Rubio-Pérez, M. Iglesias, J. Munárriz, V. Polo, J. J. Pérez-Torrente and L. A. Oro, *Chem. - A Eur. J.*, 2015, **21**, 17701–17707.

24 B. M. Choudary, C. Sridhar, M. L. Kantam and B. Sreedhar, *Tetrahedron Lett.*, 2004, **45**, 7319–7321.

25 C. E. Meyet, C. J. Pierce and C. H. Larsen, *Org. Lett.*, 2012, **14**, 964–967.

26 C. J. Pierce and C. H. Larsen, *Green Chem.*, 2012, **14**, 2672–2676.

27 P. Li, Y. Zhang and L. Wang, *Chem. - A Eur. J.*, 2009, **15**, 2045–2049.

28 W.-W. Chen, R. V Nguyen and C.-J. Li, *Tetrahedron Lett.*, 2009, **50**, 2895–2898.

29 X. Huo, J. Liu, B. Wang, H. Zhang, Z. Yang, X. She and P. Xi, *J. Mater. Chem. A*, 2013, **1**, 651–656.

30 X. Zhu and S. Chiba, *Chem. Soc. Rev.*, 2016, **45**, 4504–4523.

31 S. E. Allen, R. R. Walvoord, R. Padilla-Salinas and M. C. Kozlowski, *Chem. Rev.*, 2013, **113**, 6234–6458.

32 S. D. McCann and S. S. Stahl, *Acc. Chem. Res.*, 2015, **48**, 1756–1766.

33 C. Wei and C. J. Li, *J. Am. Chem. Soc.*, 2002, **124**, 5638–5639.

34 F. Colombo, M. Benaglia, S. Orlandi and F. Usuelli, *J. Mol. Catal. A Chem.*, 2006, **260**, 128–134.

35 E. Loukopoulos, M. Kallitsakis, N. Tsoureas, A. Abdul-Sada, N. F. Chilton, I. N. Lykakis and G. E. Kostakis, *Inorg. Chem.*, 2017, **56**, 4898–4910.

36 R. M. Clarke and T. Storr, *Dalton Trans.*, 2014, **43**, 9380–9391.

37 T. Storr, P. Verma, R. C. Pratt, E. C. Wasinger, Y. Shimazaki and T. D. P. Stack, *J. Am. Chem. Soc.*, 2008, **130**, 15448–15459.

38 K. Asami, A. Takashina, M. Kobayashi, S. Iwatsuki, T. Yajima, A. Kochem, M. Van Gastel, F. Tani, T. Kohzuma, F. Thomas and Y. Shimazaki, *Dalton Trans.*, 2014, **43**, 2283–2293.

39 A. Kochem, J. K. Molloy, G. Gellon, N. Leconte, C. Philouze, F. Berthiol, O. Jarjayes and F. Thomas, *Chem. - A Eur. J.*, 2017, **23**, 13929–13940.

40 P. G. Cozzi, *Chem. Soc. Rev.*, 2004, **33**, 410–421.

41 J. Andrez, V. Guidal, R. Scopelliti, J. Pécaut, S. Gambarelli and M. Mazzanti, *J. Am. Chem. Soc.*, 2017, **139**, 8628–8638.

42 L. Chiang, E. C. Wasinger, Y. Shimazaki, V. Young, T. Storr and T. D. P. Stack, *Inorg Chim Acta*, 2018, **481**, 151–158.

43 C. Freire and B. de Castro, *J. Chem. Soc. Dalt. Trans.*, 2002, 1491–1498.

44 P. Zanello, S. Tamburini, P. A. Vigato and G. A. Mazzocchin, *Coord. Chem. Rev.*, 1987, **77**, 165–273.

45 A. Böttcher, H. Elias, E. G. Jäger, H. Langfelderova, M. Mazur, L. Müller, H. Paulus, P. Pelikan, M. Rudolph and M. Valko, *Inorg. Chem.*, 1993, **32**, 4131–4138.

46 A. Pasini, E. Bernini, M. Scaglia and G. De Santis, *Polyhedron*, 1996, **15**, 4461–4467.

47 W. Zhang, N. Saraei, H. Nie, J. R. Vaughn, A. S. Jones, M. S. Mashuta, R. M. Buchanan and C. A. Grapperhaus, *Dalton Trans.*, 2016, **45**, 15791–15799.

48 B. Agrahari, S. Layek, R. Ganguly and D. D. Pathak, *New J. Chem.*, 2018, **42**, 13754–13762.

49 M. Tajbaksh, M. Farhang, H. R. Mardani, R. Hosseinzadeh and Y. Sarrafi, *Chinese J. Catal.*, 2013, **34**, 2217–2222.

50 S. I. Sampani, S. Aubert, M. Cattoen, K. Griffiths, A. Abdul-Sada, G. Akien, G. J. Tizzard, S. Coles, S. Arseniyadis and G. E. Kostakis, *Dalton Trans.*, 2018, **47**, 4486–4493.

51 C. Baleizão and H. Garcia, *Chem. Rev.*, 2006, **106**, 3987–4043.

52 S. Bunce, R. J. Cross, L. J. Farrugia, S. Kunchandy, L. L. Meason, K. W. Muir, M. O'Donnell, R. D. Peacock, D. Stirling and S. J. Teat, *Polyhedron*, 1998, **17**, 4179–4187.

53 W.-H. Leung, E. Y. Y. Chan, E. K. F. Chow, I. D. Williams, S.-M. Peng and C. M. Zepp, *J. Chem. Soc. Dalt. Trans.*, 1996, **15**, 1229.

54 P. Adão, S. Barroso, F. Avecilla, M. C. Oliveira and J. C. Pessoa, *J. Organomet. Chem.*, 2014, **760**, 212–223.

55 J. Cheng, K. Wei, X. Ma, X. Zhou and H. Xiang, *J. Phys. Chem. C*, 2013, **117**, 16552–16563.

56 S. Biswas, A. Dutta, M. Debnath, M. Dolai, K. K. Das and M. Ali, *Dalton Trans.*, 2013, **42**, 13210–13219.

57 R. Soengas, Y. Navarro, M. J. Iglesias and F. López-Ortiz, *Molecules*, 2018, **23**, 2975.

58 L. Shi, Y. Q. Tu, M. Wang, F. M. Zhang and C. A. Fan, *Org. Lett.*, 2004, **6**, 1001–1003.

59 J. Brussee, J. L. G. Groenendijk, J. M. te Koppele and A. C. A. Jansen, *Tetrahedron*, 1985, **41**, 3313–3319.

60 M. Smrčina, M. Lorenc, V. Hanuš, P. Sedmera and P. Kočovský, *J. Org. Chem.*, 1992, **57**, 1917–1920.

61 D. S. Peters, F. E. Romesberg and P. S. Baran, *J. Am. Chem. Soc.*, 2018, **140**, 2072–2075.

62 S. Nakamura, M. Ohara, Y. Nakamura, N. Shibata and T. Toru, *Chem. - A Eur. J.*, 2010, **16**, 2360–2362.

63 H. H. Thorp, *Inorg. Chem.*, 1992, **31**, 1585–1588.

64 F. Thomas, O. Jarjayes, C. Duboc, C. Philouze, E. Saint-Aman and J. L. Pierre, *Dalton Trans.*, 2004, 2662–2669.

65 R. C. Pratt and T. D. P. Stack, *J. Am. Chem. Soc.*, 2003, **125**, 8716–8717.

66 R. Bai, G. Zhang, H. Yi, Z. Huang, X. Qi, C. Liu, J. T. Miller, A. J. Kropf, E. E. Bunel, Y. Lan and A. Lei, *J. Am. Chem. Soc.*, 2014, **136**, 16760–16763.

67 G. Zhang, H. Yi, G. Zhang, Y. Deng, R. Bai, H. Zhang, J. T. Miller, A. J. Kropf, E. E.

Bunel and A. Lei, *J. Am. Chem. Soc.*, 2014, **136**, 924–926.

68 Z. Han, L. Shen, W. W. Brennessel, P. L. Holland and R. Eisenberg, *J. Am. Chem. Soc.*, 2013, **135**, 14659–14669.

69 S. V. Samuelsen, C. Santilli, M. S. G. Ahlquist and R. Madsen, *Chem. Sci.*, 2019, **10**, 1150–1157.

70 S. N. Semenov, L. Belding, B. J. Cafferty, M. P. S. Mousavi, A. M. Finogenova, R. S. Cruz, E. V. Skorb and G. M. Whitesides, *J. Am. Chem. Soc.*, 2018, **140**, 10221–10232.

71 A. Merk, H. Großekappenberg, M. Schmidtmann, M. P. Luecke, C. Lorent, M. Driess, M. Oestreich, H. F. T. Klare and T. Müller, *Angew. Chem. Int. Ed.*, 2018, **57**, 15267–15271.

72 E. C. Ashby, *Acc. Chem. Res.*, 1988, **21**, 414–421.

73 M. P. Plesniak, H.-M. Huang and D. J. Procter, *Nat. Rev. Chem.*, 2017, **1**, 0077.

74 M. J. Frisch, G. W. Trucks, H. B. Schlegel, G. E. Scuseria, M. A. Robb, J. R. Cheeseman, G. Scalmani, V. Barone, B. Mennucci, G. A. Petersson, H. Nakatsuji, M. Caricato, X. Li, H. P. Hratchian, A. F. Izmaylov, J. Bloino, G. Zheng, J. L. Sonnenberg, M. Hada, M. Ehara, K. Toyota, R. Fukuda, J. Hasegawa, M. Ishida, T. Nakajima, Y. Honda, O. Kitao, H. Nakai, T. Vreven, J. A., Jr. Montgomery, J. E. Peralta, F. Ogliaro, M. Bearpark, J. J. Heyd, E. Brothers, K. N. Kudin, V. N. Staroverov, R. Kobayashi, J. Normand, K. Raghavachari, A. Rendell, J. C. Burant, S. S. Iyengar, J. Tomasi, M. Cossi, N. Rega, N. J. Millam, M. Klene, J. E. Knox, J. B. Cross, V. Bakken, C. Adamo, J. Jaramillo, R. Gomperts, R. E. Stratmann, O. Yazyev, A. J. Austin, R. Cammi, C. Pomelli, J. W. Ochterski, R. L. Martin, K. Morokuma, V. G. Zakrzewski, G. A. Voth, P. Salvador, J. J. Dannenberg, S. Dapprich, A. D. Daniels, Ö. Farkas, J. B. Foresman, J. V. Ortiz, J. Cioslowski, D. J. Fox, Gaussian 09, Revision D.01; Gaussian, Inc.: Wallingford, CT, 2010.

75 J. P. Perdew, K. Burke and M. Ernzerhof, *Phys. Rev. Lett.* 1996, **77**, 3865.

76 M. Ernzerhof and G. E. Scuseria, *J. Chem. Phys.* 1999, **110**, 5029.

77 C. Adamo and V. Barone, *Chem. Phys. Lett.*, 1997, **274**, 242.

78 C. Adamo and V. Barone, *J. Chem. Phys.*, 1999 **110**, 6160.

79 C. Adamo, G. E. Scuseria and V. Barone, *J. Chem. Phys.* 1999, **111**, 2889.

80 C. Adamo and V. Barone, V. *Theor. Chem. Acc.* 2000, **105**, 169.

81 V. Vetere, C. Adamo and P. Maldivi, *Chem. Phys. Lett.* 2000, **325**, 99.

82 F. Weigend and R. Ahlrichs, *Phys. Chem. Chem. Phys.* 2005, **7**, 3297.

83 EMSL basis set exchange, https://bse.pnl.gov/bse/portal, accessed 26-06-2015.

84 A. E. Reed, L. A. Curtiss and F. Weinhold, *Chem. Rev.*, 1998, **88**, 899.

85 F. Weinhold, In *The Encyclopedia of Computational Chemistry*; Schleyer, P. v. R., Ed.; Wiley: Chichester, U.K., 1998; p 1792.

86 *NBO 6.0.* E. D. Glendening, J.K. Badenhoop, A. E. Reed, J. E. Carpenter, J. A. Bohmann, C. M. Morales, C. R. Landis and F.Weinhold, Theoretical Chemistry Institute, University of Wisconsin, Madison.

87 J. Tomasi, B. Mennucci and R. Cammi, *Chem. Rev.* 2005, **105**, 2999.

88 S. J. Coles and P. A. Gale, *Chem. Sci.*, 2012, **3**, 683–689.

Graphical Abstract